



Contents lists available at ScienceDirect

Biochemical and Biophysical Research Communications

journal homepage: [www.elsevier.com/locate/ybbrc](http://www.elsevier.com/locate/ybbrc)



# Development and characterization of a hydrogen peroxide-resistant cholangiocyte cell line: A novel model of oxidative stress-related cholangiocarcinoma genesis



Raynoo Thanan<sup>a, b</sup>, Anchalee Techasen<sup>b, c</sup>, Bo Hou<sup>d</sup>, Wassana Jamnongkan<sup>a, b</sup>,  
Napart Armartmuntree<sup>a, b</sup>, Puangrat Yongvanit<sup>a, b, \*</sup>, Mariko Murata<sup>d, \*\*</sup>

<sup>a</sup> Department of Biochemistry, Faculty of Medicine, Khon Kaen University, Khon Kaen 40002, Thailand

<sup>b</sup> Liver Fluke and Cholangiocarcinoma Research Center, Faculty of Medicine, Khon Kaen University, Khon Kaen 40002, Thailand

<sup>c</sup> Faculty of Associated Medical Science, Khon Kaen University, Khon Kaen 40002, Thailand

<sup>d</sup> Department of Environmental and Molecular Medicine, Mie University Graduate School of Medicine, Tsu, Mie 514-8507, Japan

## ARTICLE INFO

### Article history:

Received 12 June 2015

Accepted 17 June 2015

Available online 20 June 2015

### Keywords:

Oxidative stress

Cholangiocarcinoma

Resistant-cells

Epigenetics

Anti-oxidants

## ABSTRACT

Oxidative stress is a cause of inflammation-related diseases, including cancers. Cholangiocarcinoma is a liver cancer with bile duct epithelial cell phenotypes. Our previous studies in animal and human models indicated that oxidative stress is a major cause of cholangiocarcinoma development. Hydrogen peroxide ( $H_2O_2$ ) can generate hydroxyl radicals, which damage lipids, proteins, and nucleic acids, leading to cell death. However, some cells can survive by adapting to oxidative stress conditions, and selective clonal expansion of these resistant cells would be involved in oxidative stress-related carcinogenesis. The present study aimed to establish  $H_2O_2$ -resistant cell line from an immortal cholangiocyte cell line (MMNK1) by chronic treatment with low-concentration  $H_2O_2$  (25  $\mu$ M). After 72 days of induction,  $H_2O_2$ -resistant cell lines (ox-MMNK1-L) were obtained. The ox-MMNK1-L cell line showed  $H_2O_2$ -resistant properties, increasing the expression of the anti-oxidant genes catalase (CAT), superoxide dismutase-1 (SOD1), superoxide dismutase-2 (SOD2), and superoxide dismutase-3 (SOD3) and the enzyme activities of CAT and intracellular SODs. Furthermore, the resistant cells showed increased expression levels of an epigenetics-related gene, DNA methyltransferase-1 (DNMT1), when compared to the parental cells. Interestingly, the ox-MMNK1-L cell line had a significantly higher cell proliferation rate than the MMNK1 normal cell line. Moreover, ox-MMNK1-L cells showed pseudopodia formation and the loss of cell-to-cell adhesion (multi-layers) under additional oxidative stress (100  $\mu$ M  $H_2O_2$ ). These findings suggest that  $H_2O_2$ -resistant cells can be used as a model of oxidative stress-related cholangiocarcinoma genesis through molecular changes such as alteration of gene expression and epigenetic changes.

© 2015 Elsevier Inc. All rights reserved.

## 1. Introduction

Oxidative stress is a major cause of inflammation-related diseases, including cancer [1]. Overproduction of reactive oxygen species (ROS) and reactive nitrogen species (RNS) can damage lipids, proteins, and nucleic acids [1]. ROS damage lipids, leading to chain reactions of lipid peroxidation and formation of oxysterols,

and consequently to carbonyl protein formation and etheno-DNA adducts [2,3]. RNS and ROS can also directly oxidize DNA, causing oxidation products such as the 8-nitroguanine and 8-hydroxy-2'-deoxyguanosine (also known as 8-oxodG) [4], which are mutagenic lesions that can induce point mutations [1]. Recently, many literature reviews have suggested that oxidative stress is also involved in genetic instability, epigenetic changes, and alteration of gene expression [1,5–7].

The etiologies of cholangiocarcinoma have been identified as diseases that damage the bile duct and liver, such as primary sclerosing cholangitis, Caroli's disease, congenital choledochal cysts, hepatitis C virus infection, and liver fluke infections [8,9]. The highest incidence of cholangiocarcinoma is found in northeastern

\* Corresponding author. Department of Biochemistry, Faculty of Medicine, Khon Kaen University, Khon Kaen 40002, Thailand.

\*\* Corresponding author.

E-mail addresses: [puangrat@kku.ac.th](mailto:puangrat@kku.ac.th) (P. Yongvanit), [mmurata@doc.medic.mie-u.ac.jp](mailto:mmurata@doc.medic.mie-u.ac.jp) (M. Murata).

Thailand, where liver fluke (*Opisthorchis viverrini*) infection is endemic [10]. Oxidative damage to biomolecules is key events in opisthorchiasis-driven cholangiocarcinoma genesis [11]. Our previous studies demonstrated that the etheno-DNA adducts, 8-nitroguanine and 8-oxodG were formed in the epithelial cells of normal and hyperplastic bile ducts of *O. viverrini*-infected hamster liver tissues [12,13]. Moreover, 8-oxodG and other etheno-DNA adducts were also detected high levels in urine from *O. viverrini*-infected subjects and cholangiocarcinoma patients [12,14]. Significant formation of carbonylated proteins was also found in cholangiocarcinoma tissues [15]. Oxysterols, a kind of oxidized cholesterol, were also detected in cholangiocarcinoma tissues. Our recent study demonstrated that anti-apoptosis was significantly increased in an immortal cholangiocyte cell line (MMNK1) that was exposed long-term to the oxysterols cholestan-3- $\beta$ ,5- $\alpha$ ,6- $\beta$ -triol (Triol) and 3-keto-cholest-4-ene (3K4) [16]. In general, oxidative stress-damaged cells eventually undergo cell apoptosis or necrosis, whereas damaged cells that can survive under oxidative stress conditions may play important roles in the pathological effect of inflammation-related cancer development.

Hydrogen peroxide ( $H_2O_2$ ) can generate highly reactive hydroxyl radicals in the presence of metal ions via Fenton-like reactions, resulting in oxidative damage to cellular biomolecules. Additionally, unsaturated fatty acids can be oxidized and consequently produce superoxide anions and hydroxyl radicals in the presence of  $Fe^{2+}$  [17]. Chronic treatment of mammalian cells with  $H_2O_2$  has shown that cells are able to adapt to oxidative stress [18–22]. The most common resistance mechanisms are based on an increase in the activity of anti-oxidative enzymes such as catalase (CAT) and superoxide dismutases (SODs), as well as glutathione (GSH) content [18–22]. CAT is a  $H_2O_2$  specific antioxidant enzyme that converts  $H_2O_2$  to water and oxygen [23]. SODs are antioxidant enzymes that catalyze superoxide anion radicals to  $H_2O_2$ . SOD1 (CuZn-SOD) localizes at the cytoplasm whereas SOD2 (Mn-SOD) and SOD3 (EC-SOD) localize at the mitochondrial matrix and extracellularly, respectively [24]. Identification of novel defense mechanisms against oxidative stress could lead to the development of new drug targets for the treatment of cholangiocarcinoma.

In this study, we aimed to develop and characterize a  $H_2O_2$ -resistant cell line from an immortal normal cholangiocyte cell line (MMNK1). MMNK1 parental cells were treated daily with low-concentration  $H_2O_2$  (25  $\mu$ M, one-third of the 50% inhibitory concentration (IC50) value by 48-hr cytotoxicity assay) for 72 days. We analyzed the anti-oxidant properties (GSH content and gene expression levels of CAT, SOD1, SOD2, and SOD3 as well as the enzyme activities of CAT and SODs) and epigenetic regulation by DNA methyltransferase-1 (DNMT1) gene expression. Cell proliferation and wound healing assays were performed to characterize the resistant cell line compared with their parental cells.

## 2. Materials and methods

### 2.1. Cell culture

The immortalized human cholangiocyte MMNK1 (also known as MMNK-1) cell line was supplied by Professor Naoya Kobayashi (Okayama University, Japan). MMNK1 was established from SV40T-transduced human liver OUMS-21 cells using serial transfection of simian virus 40 large T (SV40T) followed by human telomerase reverse transcriptase (hTERT) [25]. Cells were cultured in Hams F12 (Invitrogen, CA, USA) supplemented with 10% fetal calf serum, 100 U/mL penicillin, and 0.1 mg/mL streptomycin or 0.1 mg/mL kanamycin at 37 °C in 5%  $CO_2$ . The culture medium was changed every 48 h.

### 2.2. Induction of a cholangiocyte cell line exposed daily to low doses of hydrogen peroxide

MMNK1 cells were treated daily with 25  $\mu$ M  $H_2O_2$  for 15 passages. Briefly, MMNK1 cells ( $5 \times 10^5$  cells) were seeded overnight in a 100-mm<sup>2</sup> petri dish with 10 mL Ham F12 complete medium. After that,  $H_2O_2$  was added to the culture dish to a final concentration of 25  $\mu$ M. Every 24 h, a new aliquot of  $H_2O_2$  was added and the culture medium was changed every 48 h until cells reached about 80–90% confluence; this entire phase was treated as the 1st passages. The cells were then harvested by trypsinization and seeded in a new culture dish for the 2nd passages of treatment with 25  $\mu$ M  $H_2O_2$  every 24 h. A total of 15 passages were performed over 72 days. The  $H_2O_2$ -resistant cells were named ox-MMNK1-L. The established cells were maintained by culture in Ham F12 complete medium without  $H_2O_2$ , and aliquots of living cells were stored in 10% DMSO containing fetal calf serum in liquid nitrogen.

### 2.3. Hydrogen peroxide cytotoxicity assay

Cytotoxicity in Ham F12 complete medium containing various  $H_2O_2$  concentrations for 48 h was analyzed using a tetrazolium (MTT)-based assay. Briefly, suspensions of MMNK1 and ox-MMNK1-L cells in Ham F12 complete medium were seeded in 96-well plates at  $1.5 \times 10^3$  cells per well. The culture medium was removed after 24-h incubation. Ham F12 complete medium containing various concentrations of  $H_2O_2$  (0, 12.5, 25, 50, 100, 200, 300, 400  $\mu$ M) was added and the cells were continuously cultured for 24 h. After that, the culture medium was removed and new complete medium containing various concentrations of  $H_2O_2$  was added and the culture was continued for another 24 h. Finally, relative cell numbers (%) were analyzed by the standard MTT assay protocol. The IC50 of daily treatment with  $H_2O_2$  at 48 h for each cell type was also calculated.

An additional  $5 \times 10^5$  MMNK1 and ox-MMNK1-L cells suspended in Ham F12 complete medium were seeded in 100-mm<sup>2</sup> culture dishes and incubated at 37 °C in 5%  $CO_2$  overnight. After that,  $H_2O_2$  was added to the culture dish at a final concentration of 100  $\mu$ M. Every 24 h, a new aliquot of  $H_2O_2$  was added and the culture medium was changed every 48 h. Cell growth and morphology were observed under an inverted microscope.

### 2.4. Collection of cell pellets

MMNK1 and ox-MMNK1-L cell lines were cultured in 10-mm<sup>2</sup> petridishes containing Ham F12 complete medium, the medium was changed every 48 h until 80–90% confluence was achieved, then cells were harvested by trypsinization. Cell pellets were washed twice with cold PBS and stored at –80 °C until used.

### 2.5. Measurement of CAT, SOD1, SOD2, SOD3, and DNMT1 mRNA expression levels by real-time PCR

CAT, SOD1, SOD2, SOD3, and DNMT1 mRNA expression levels were analyzed with the ABI Step One Plus Real-time PCR System (Applied Biosystems, Singapore) using TaqMan Probes (CAT, Hs00156308\_m1; SOD1, Hs00916176\_m1; SOD2, Hs01553554\_m1; SOD3, Hs00162090\_m1; DNMT1, Hs00945899\_m1 and  $\beta$ -actin, Hs99999903\_m1, Applied Biosystems, Foster City, CA, USA). Briefly, total RNA was isolated from MMNK1 and ox-MMNK1-L cell pellets with Trizol<sup>®</sup> reagent (Invitrogen, CA, USA) following the manufacturer's protocol. For the reverse transcription reaction, 1  $\mu$ g total RNA was converted to

cDNA using the High Capacity RNA-to-cDNAKit (Applied Biosystems). The PCR reaction was performed using TaqMan® Gene Expression Master Mix (Applied Biosystems) following the manufacturer's protocol. Relative mRNA expressions (fold changes) were analyzed with a cycle threshold (Ct) in the linear range of amplification and then processed by Relative Expression Quantification (REQ) using  $\beta$ -actin as an internal control.

## 2.6. Measurement of CAT activity

Cells growth at 80–90% confluent in Ham F12 complete medium were washed twice with cold PBS then cells were harvested by scraping in 1 mL cold Assay buffer (DetectX® Catalase Colorimetric Activity Kit, Arbor Assays, MI, USA). Then cells were homogenized by Omni bead ruptor 24 (OMNI International<sup>IM</sup>, GA, USA). The

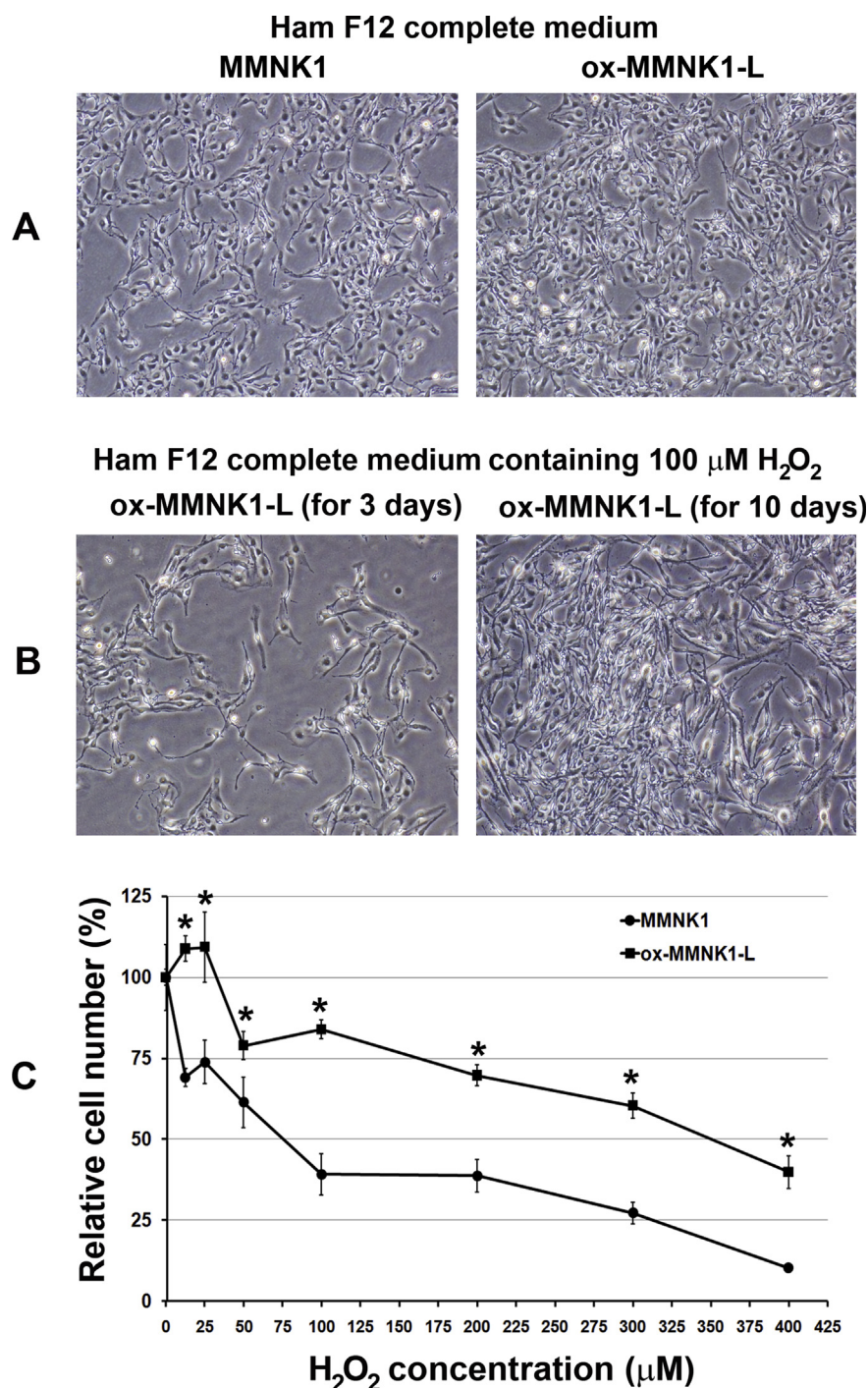


**Fig. 1.** Cell morphologies of MMNK1 and ox-MMNK1-L cell lines and  $H_2O_2$  cytotoxicity. (A) Morphology of MMNK1 and ox-MMNK1-L cells incubated in Ham F12 complete medium (no  $H_2O_2$ ) for 4 days. (B) Morphology of ox-MMNK1-L cells incubated in Ham F12 complete medium containing 100  $\mu$ M  $H_2O_2$  for 3 and 10 days, respectively. Original magnification was 200 $\times$ . (C) Cytotoxicity of MMNK1 ( $n = 3$ ) and ox-MMNK1-L ( $n = 3$ ) cells incubated in Ham F12 complete medium containing various concentrations of  $H_2O_2$  for 48 h \* indicates  $p < 0.05$  analyzed by Student's  $t$  test when compared with MMNK1 parental cells.



homogenized cells were centrifuged at 12,000 rpm, 4 °C for 5 min then the supernatants were collected. After that, CAT enzyme activity was measured by DetectX<sup>®</sup> Catalase Colorimetric Activity Kit (Arbor Assays) using the manual protocol. Protein concentrations were determined by Pierce<sup>®</sup> BCA Protein Assay Kit (Pierce Biotechnology, IL, USA). The CAT enzyme activities were finally calculated as U/mg proteins.

### 2.7. Measurement of intracellular SODs activities

The fresh cell pellets were homogenized by Omni bead ruptor 24 (OMNI International<sup>™</sup>) in 500  $\mu$ L cold PBS. The homogenized cells were centrifuged at 12,000 rpm, 4 °C for 5 min then the supernatants were collected. After that, SODs enzyme activities was measured by DetectX<sup>®</sup> Superoxide Dismutase (SOD) Colorimetric Activity Kit (Arbor Assays) using the manual protocol. Protein concentrations were determined by Pierce<sup>®</sup> BCA Protein Assay Kit (Pierce Biotechnology). The SODs enzyme activities were finally calculated as U/mg proteins.

### 2.8. Measurement of GSH levels by high-pressure liquid chromatography–electrochemical detection (HPLC-ECD)

GSH levels in MMNK1 and ox-MMNK1-L cells were measured (quadruplicate) by an HPLC-ECD system. Briefly, pellets containing  $5 \times 10^5$  cells were re-suspended in 50  $\mu$ L PBS containing 5% (w/v) TCA and then homogenized by an ultrasonicator (SONIFIER 450) at 50 W output for 15 s. The tubes were centrifuged at 20,000 g for 30 min at 4 °C. Then, supernatants were collected for GSH measurement using an HPLC-ECD system (Eicom, Kyoto, Japan) as described previously [26], to detect the SH-containing compounds compared with GSH standard solution. Additionally, other aliquots of  $5 \times 10^5$  cell pellets were collected for total protein detection by Coomassie reagent compared with standard albumin solution. The GSH levels were calculated as pmol/ $\mu$ g protein.

### 2.9. Cell proliferation assay

Cell proliferation was determined by sulforhodamine B colorimetric (SRB) assay. A total of  $1.5 \times 10^3$  of MMNK1 and ox-MMNK1-L cells were seeded in a 96-well plate. Cells were fixed with 10% (w/v) trichloroacetic acid for another 1, 2, 3, or 4 days of culture. After washing and air drying, SRB was added and cells were incubated for 1 h. Excess dye was removed by washing repeatedly with 1% (v/v) acetic acid. The protein-bound dye was dissolved in 10 mM Tris-based solution for optical density (OD) determination at 540 nm using a microplate reader.

### 2.10. Wound healing assay

MMNK1 and ox-MMNK1-L cells were seeded in 24-well plates. Upon reaching over confluence, the wound was incised by scratching cell monolayers using a 200- $\mu$ L pipette tip. Photographs were taken under phase contrast microscopy at 0–48 h and the degrees of migration were compared among cell types.

## 3. Results

### 3.1. Cells morphology and acquisition of resistance to hydrogen peroxide cytotoxicity

After cell growth in Ham F12 complete medium (no H<sub>2</sub>O<sub>2</sub>) for 4 days, MMNK1 and ox-MMNK1-L cell morphologies were captured by an inverted microscope as shown in Fig. 1A. The parental MMNK1 cells had a spindle-shaped morphology. ox-MMNK1-L

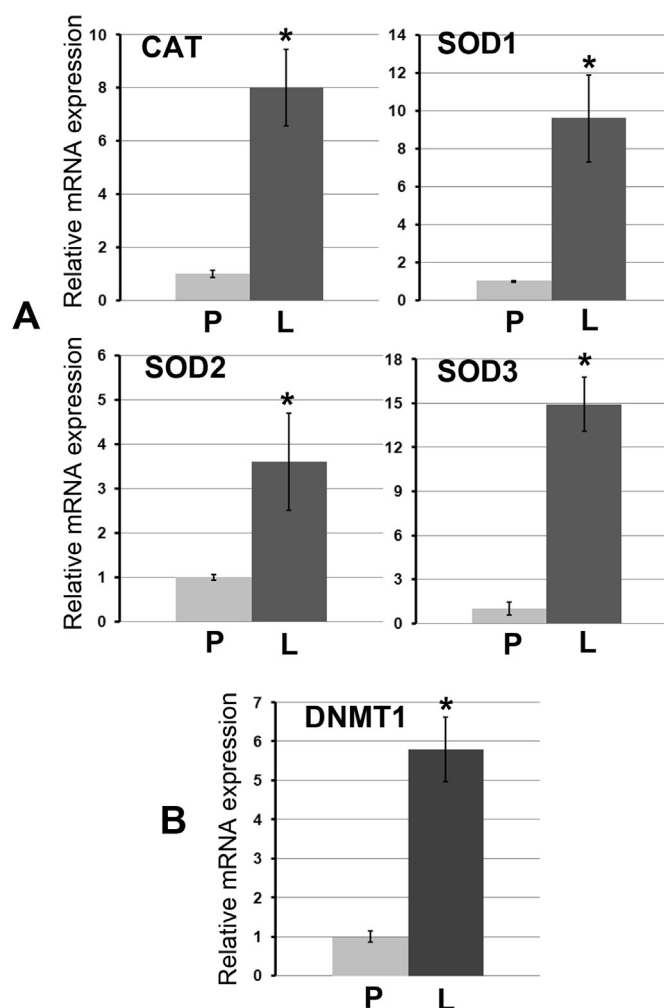


**Fig. 2.** Relative mRNA expression levels of CAT, SOD1, SOD2, SOD3 and DNMT1. (A) Relative mRNA expression levels were measured by real-time PCR for the antioxidant enzymes catalase (CAT), superoxide dismutase-1 (SOD1), superoxide dismutase-2 (SOD2), and superoxide dismutase-3 (SOD3), and adjusted by  $\beta$ -actin mRNA expression. (B) Relative mRNA expression of DNMT1 adjusted by  $\beta$ -actin mRNA expression. P = MMNK1 parental cells, L = ox-MMNK1-L cells, \* indicates  $p < 0.05$  analyzed by Student's t test when compared with MMNK1 parental cells.

cells in normal culture medium were morphologically similar to MMNK1 cells. However, the morphologies of ox-MMNK1-L cells were changed following daily treatment with 100  $\mu$ M H<sub>2</sub>O<sub>2</sub> at 3 and 10 days in Ham F12 complete medium, as shown in Fig. 1B.

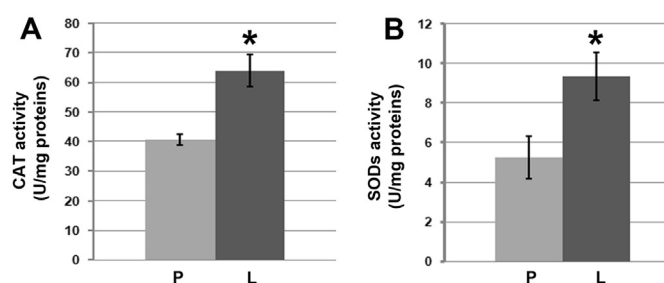


**Fig. 3.** Enzyme activities of CAT and SODs in MMNK1 and ox-MMNK1-L cells. Activities of (A) CAT and (B) SODs were determined as described in kit protocol provided by the producer. Data were normalized against total protein content in each sample. P = MMNK1 parental (n = 3) cells, L = ox-MMNK1-L cells (n = 3), \* indicates  $p < 0.05$  analyzed by Student's t test when compared with MMNK1 parental cells.

The formation of pseudopodia was increased in ox-MMNK1-L cells grown in culture medium containing 100  $\mu\text{M}$   $\text{H}_2\text{O}_2$ . At 10 days after daily treatment with  $\text{H}_2\text{O}_2$ , loss of cell-to-cell adhesion (multi-layers) was observed. In contrast, all parental MMNK1 cells died at 3 days after daily treatment with 100  $\mu\text{M}$   $\text{H}_2\text{O}_2$  (data not shown).

Fig. 1C shows the cytotoxicity caused by daily treatment of MMNK1 and ox-MMNK1-L cells with various concentrations of  $\text{H}_2\text{O}_2$  for 48 h ox-MMNK1-L cells showed a significantly higher relative number of viable cells when cultured with Ham F12 complete medium containing 0, 12.5, 25, 50, 100, 200, 300, and 400  $\mu\text{M}$   $\text{H}_2\text{O}_2$  in comparison with MMNK1 cells. Moreover, the  $\text{IC}_{50}$  for ox-MMNK1-L cells was 350  $\mu\text{M}$   $\text{H}_2\text{O}_2$  whereas that for MMNK1 cells was 75  $\mu\text{M}$   $\text{H}_2\text{O}_2$ . These results indicated that the established ox-MMNK1-L cells were resistant to  $\text{H}_2\text{O}_2$  when compared with the parental cells.

### 3.2. Anti-oxidant properties of hydrogen peroxide-resistant cell line

CAT, SOD1, SOD2, and SOD3 mRNA levels were significantly increased in ox-MMNK1-L cells compared to MMNK1 cells, as shown in Fig. 2A. Cellular CAT and SODs enzyme activities were also significantly increased in the oxidative stress resistant-cells compared to the parental cells as shown in Fig. 3. However, GSH levels were not significantly different between the two cell lines

(MMNK1 =  $11.06 \pm 1.07$  and ox-MMNK1-L =  $11.51 \pm 0.76$  pmol/ $\mu\text{g}$  protein).

### 3.3. DNMT1 expression in hydrogen peroxide-resistant cell line

ox-MMNK1-L cells showed significantly increased mRNA expression levels of DNMT1 compared with MMNK1 parental cells, as shown in Fig. 2B.

### 3.4. Cell proliferation and wound healing

Cell proliferation was significantly increased in ox-MMNK1-L cells at days 2, 3, and 4 after being cultured with Ham F12 complete medium (no  $\text{H}_2\text{O}_2$ ) compared to MMNK1 cells, as shown in Fig. 4. However, ox-MMNK1-L cells did not induce wound-healing properties when compared to the parental cells (data not shown).

## 4. Discussion

We could successfully induce and generate  $\text{H}_2\text{O}_2$ -resistant cells from an immortal cholangiocyte cell line with simple and useful protocols. ox-MMNK1-L cells had increased anti-oxidant properties via over-expression of CAT, SOD1, SOD2, and SOD3 genes, which reflect well with CAT and SODs enzymes activities. Interestingly, ox-MMNK1-L cells also demonstrated increased cell proliferation when compared to the parental cells. While conducting the

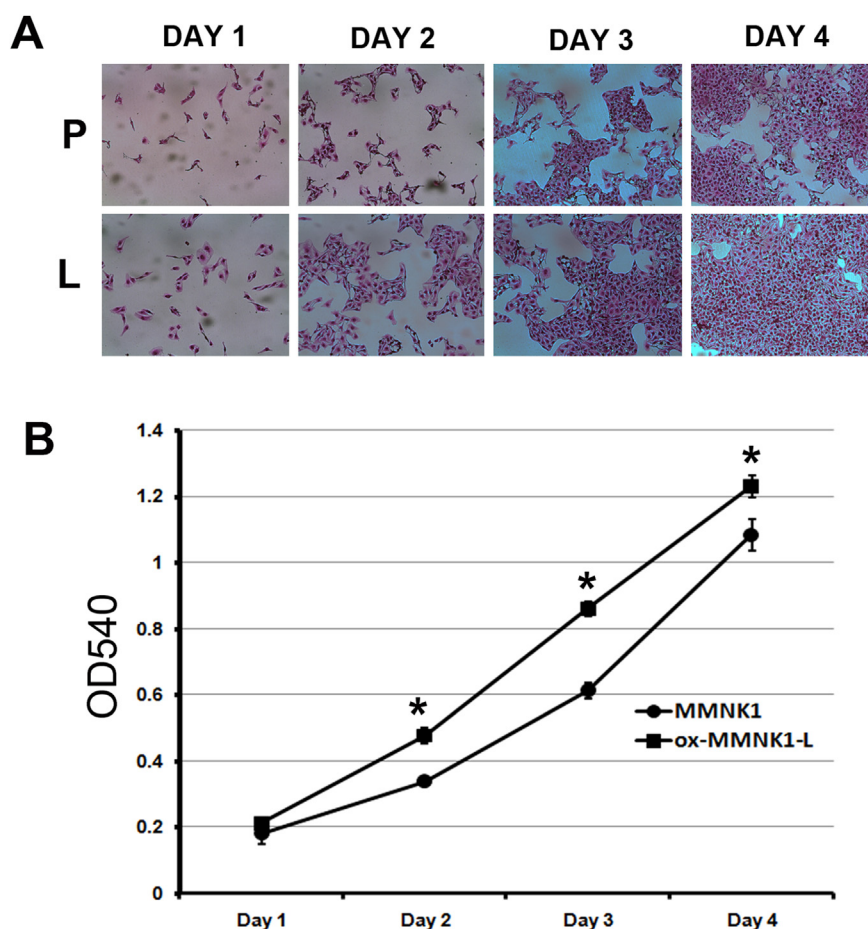


**Fig. 4.** Cell proliferation analysis of MMNK1 and ox-MMNK1-L cell lines. (A) After 1 h of SRB treatment, cells were observed with an inverted microscope at 200 $\times$  magnification. (B) Graph represents OD540 of SRB-stained cells after they were dissolved with Tris-based solution. Values are presented as mean ( $n = 3$ )  $\pm$  SD. P = MMNK1 parental cells, L = ox-MMNK1-L cells, \* indicates  $p < 0.05$  analyzed by Student's  $t$  test when compared with MMNK1 parental cells.

experiments, we evaluated the anti-oxidant properties after every 5 passage of H<sub>2</sub>O<sub>2</sub> treatment. At 15 treatment passages, the anti-oxidant properties were significantly increased; at this time we analyzed the cells with H<sub>2</sub>O<sub>2</sub>-resistant properties, DNMT1 expression levels, and cell proliferation, and performed the wound-healing assay. We also tried to treat cells with gradually increasing H<sub>2</sub>O<sub>2</sub> concentrations every passage (from 25  $\mu$ M to 70  $\mu$ M). However, at higher H<sub>2</sub>O<sub>2</sub> concentrations (70  $\mu$ M), cells were highly damaged and were close to death. On the contrary, cells treated with 25  $\mu$ M H<sub>2</sub>O<sub>2</sub> gradually adapted to H<sub>2</sub>O<sub>2</sub> and remained viable. Based on our results, we recommend that generation of H<sub>2</sub>O<sub>2</sub>-induced resistant cell lines used a protocol in which the daily H<sub>2</sub>O<sub>2</sub> treatment is one-third of the IC<sub>50</sub> concentration, and this may be easily applied to other cell types.

Epigenetics is a gene regulation system that does not involve changes in the genetic sequence; it includes processes such as DNA methylation and histone modification. DNMT1 is involved in epigenetic regulation via DNA methylation. DNMT1 catalyzes the transfer of the methyl group from S-adenosyl methionine to the cytosine base at CpG. DNA hypermethylation in promoter CpG islands may lead to gene silencing. In mice exposed to air pollution with ambient particulate matter <2.5  $\mu$ m in diameter, there were increases in DNMT1 expression as well as ROS production and methylation of the P16 promoter region [27]. Moreover, ROS induced DNMT1 activity with the cooperation of MBD4, which is involved in controlling gene expression and responding to oxidative stress [28]. However, oxidative stress is also known to induce DNA hypomethylation via oxidatively damaged DNA such as 8-oxodG and O<sup>6</sup>-methylguanine, and point mutations can interfere with the binding of DNMTs, suggesting that oxidative stress can lead to hypomethylation by inhibiting methylation of adjacent cytosine molecules [5]. The present study indicates that long-term exposure to H<sub>2</sub>O<sub>2</sub> can induce DNMT1 expression, suggesting that epigenetic changes play important roles in the oxidative stress response.

Sustaining proliferative signaling, evading growth suppressors, resisting cell death, enabling replicative immortality, inducing angiogenesis, and activating invasion and metastasis are hallmarks of cancer [29]. Mutations, genetic instability, and epigenetic changes occur in many types of cancer cells, indicating that cancer is a disease of genes [30]. Cancer cells also have stem cell properties such as sustained proliferative signaling, cell-death resistance, replicative immortality, and cell differentiation, suggesting that cancer is a disease of stem cells [31]. However, many types of cancer share common steps in carcinogenesis, including tumor initiation (fixed mutation), tumor promotion (unlimited cell proliferation), and tumor progression (invasion and metastasis). Oxidative stress clearly involves mutations through formation of mutagenic DNA lesions, suggesting that it induces tumor initiation. Our oxidative stress-resistant cell line produced from an immortal cholangiocyte cell line showed higher proliferation than the parental cell line. Interestingly, ox-MMNK1-L cells showed the formation of pseudopodia and the loss of cell-to-cell adhesion (multi-layers) under additional oxidative stress. These changes are typical of the epithelial-to-mesenchymal transition [32,33]. Taken together, our results indicate that ox-MMNK1-L cells have acquired several properties of cancer cells.

The present study shows that while MMNK1 parental cells were sensitive to H<sub>2</sub>O<sub>2</sub> (IC<sub>50</sub> = 75  $\mu$ M), ox-MMNK1-L cells were H<sub>2</sub>O<sub>2</sub>-resistant (IC<sub>50</sub> = 350  $\mu$ M). Moreover, the ox-MMNK1-L cell line could grow in culture medium containing 100  $\mu$ M H<sub>2</sub>O<sub>2</sub>, whereas the parental cells failed to proliferate. The H<sub>2</sub>O<sub>2</sub> resistance of the ox-MMNK1-L cell line was due to increased expression of anti-oxidant genes, including CAT, SOD1, SOD2, and SOD3, as compared to the parental cells. Interestingly, the ox-MMNK1-L cell line showed significantly increased cell proliferation and DNMT1

expression levels compared with the parental cells. Therefore, these H<sub>2</sub>O<sub>2</sub>-resistant cells can be used as a novel model for the molecular study of oxidative stress-related alterations of gene expression, epigenetic changes, and drug targeting in cholangiocarcinoma.

## Acknowledgments

This study was partly supported by Thailand Research Fund (TRG5680039) to RT; the Higher Education Research Promotion and National Research University Project of Thailand, Office of the Higher Education Commission, through the Center of Excellence in Specific Health Problems in the Greater Mekong Sub-region cluster (SHeP-GMS), Khon Kaen University to PY (NRU542010); and a Grant-in-Aid for Scientific Research from the Ministry of Education, Culture, Sports, Science and Technology of Japan (No. 25293149) to MM.

## Transparency document

Transparency document related to this article can be found online at <http://dx.doi.org/10.1016/j.bbrc.2015.06.112>.

## References

- [1] R. Thanan, S. Oikawa, Y. Hiraku, S. Ohnishi, N. Ma, S. Pinlaor, P. Yongvanit, S. Kawanishi, M. Murata, Oxidative stress and its significant roles in neurodegenerative diseases and cancer, *Int. J. Mol. Sci.* 16 (2014) 193–217.
- [2] G. Barrera, Oxidative stress and lipid peroxidation products in cancer progression and therapy, *ISRN Oncol.* 2012 (2012) 137289.
- [3] T.T. Reed, Lipid peroxidation and neurodegenerative disease, *Free Radic. Biol. Med.* 51 (2011) 1302–1319.
- [4] S. Kawanishi, Y. Hiraku, S. Oikawa, Mechanism of guanine-specific DNA damage by oxidative stress and its role in carcinogenesis and aging, *Mutat. Res.* 488 (2001) 65–76.
- [5] R. Franco, O. Schoneveld, A.G. Georgakilas, M.I. Panayiotidis, Oxidative stress, DNA methylation and carcinogenesis, *Cancer Lett.* 266 (2008) 6–11.
- [6] M. Murata, R. Thanan, N. Ma, S. Kawanishi, Role of nitrate and oxidative DNA damage in inflammation-related carcinogenesis, *J. Biomed. Biotechnol.* 2012 (2012) 623019.
- [7] N. Nishida, M. Kudo, Oxidative stress and epigenetic instability in human hepatocarcinogenesis, *Dig. Dis.* 31 (2013) 447–453.
- [8] S.A. Khan, H.C. Thomas, B.R. Davidson, S.D. Taylor-Robinson, Cholangiocarcinoma, *Lancet* 366 (2005) 1303–1314.
- [9] G.L. Tyson, H.B. El-Serag, Risk factors for cholangiocarcinoma, *Hepatology* 54 (2011) 173–184.
- [10] V. Vatanasapt, S. Sriamporn, P. Vatanasapt, Cancer control in Thailand, *Jpn. J. Clin. Oncol.* 32 (Suppl.) (2002) S82–S91.
- [11] P. Yongvanit, S. Pinlaor, H. Bartsch, Oxidative and nitrate DNA damage: key events in opisthorchiasis-induced carcinogenesis, *Parasitol. Int.* 61 (2012) 130–135.
- [12] S. Dechakhamphu, P. Yongvanit, J. Nair, S. Pinlaor, P. Sithithaworn, H. Bartsch, High excretion of etheno adducts in liver fluke-infected patients: protection by praziquantel against DNA damage, *Cancer Epidemiol. Biomarkers Prev.* 17 (2008) 1658–1664.
- [13] S. Pinlaor, N. Ma, Y. Hiraku, P. Yongvanit, R. Semba, S. Oikawa, M. Murata, B. Sripa, P. Sithithaworn, S. Kawanishi, Repeated infection with *Opisthorchis viverrini* induces accumulation of 8-nitroguanine and 8-oxo-7,8-dihydro-2'-deoxyguanine in the bile duct of hamsters via inducible nitric oxide synthase, *Carcinogenesis* 25 (2004) 1535–1542.
- [14] R. Thanan, M. Murata, S. Pinlaor, P. Sithithaworn, N. Khuntikeo, W. Tangkanakul, Y. Hiraku, S. Oikawa, P. Yongvanit, S. Kawanishi, Urinary 8-oxo-7,8-dihydro-2'-deoxyguanosine in patients with parasite infection and effect of antiparasitic drug in relation to cholangiocarcinogenesis, *Cancer Epidemiol. Biomarkers Prev.* 17 (2008) 518–524.
- [15] R. Thanan, S. Oikawa, P. Yongvanit, Y. Hiraku, N. Ma, S. Pinlaor, C. Pairojkul, C. Wongkham, B. Sripa, N. Khuntikeo, S. Kawanishi, M. Murata, Inflammation-induced protein carbonylation contributes to poor prognosis for cholangiocarcinoma, *Free Radic. Biol. Med.* 52 (2012) 1465–1472.
- [16] A. Jusakul, W. Loilome, N. Namwat, A. Techasen, R. Kuver, G.N. Ioannou, C. Savard, W.G. Haigh, P. Yongvanit, Anti-apoptotic phenotypes of cholestan-3 $\beta$ ,5 $\alpha$ ,6 $\beta$ -triol-resistant human cholangiocytes: characteristics contributing to the genesis of cholangiocarcinoma, *J. Steroid Biochem. Mol. Biol.* 138 (2013) 368–375.
- [17] Y. Kambayashi, S. Tero-Kubota, Y. Yamamoto, M. Kato, M. Nakano, K. Yagi, K. Ogino, Formation of superoxide anion during ferrous ion-induced

- decomposition of linoleic acid hydroperoxide under aerobic conditions, *J. Biochem.* 134 (2003) 903–909.
- [18] O. Cantoni, A. Guidarelli, P. Sestili, F. Mannello, G. Gazzanelli, F. Cattabeni, Development and characterization of hydrogen peroxide-resistant Chinese hamster ovary cell variants—I. Relationship between catalase activity and the induction/stability of the oxidant-resistant phenotype, *Biochem. Pharmacol.* 45 (1993) 2251–2257.
- [19] A. Spector, R.R. Wang, W. Ma, N.J. Kleiman, Development and characterization of an H<sub>2</sub>O<sub>2</sub>-resistant immortal lens epithelial cell line, *Invest Ophthalmol. Vis. Sci.* 41 (2000) 832–843.
- [20] K. Bose Girigoswami, G. Bhaumik, R. Ghosh, Induced resistance in cells exposed to repeated low doses of H<sub>2</sub>O<sub>2</sub> involves enhanced activity of anti-oxidant enzymes, *Cell. Biol. Int.* 29 (2005) 761–767.
- [21] D.R. Spitz, S.J. Sullivan, The generation of stable oxidative stress-resistant phenotypes in Chinese hamster fibroblasts chronically exposed to hydrogen peroxide or hyperoxia, *Methods Mol. Biol.* 610 (2010) 183–199.
- [22] A.E. Maczurek, R. Wild, D. Laurenti, M.L. Steele, L. Ooi, G. Munch, Generation of hydrogen peroxide-resistant murine neuroblastoma cells: a target discovery platform for novel neuroprotective genes, *J. Neural Transm.* 120 (2013) 1171–1178.
- [23] H. Sies, T. Bucher, N. Oshino, B. Chance, Heme occupancy of catalase in hemoglobin-free perfused rat liver and of isolated rat liver catalase, *Arch. Biochem. Biophys.* 154 (1973) 106–116.
- [24] I.N. Zelko, T.J. Mariani, R.J. Folz, Superoxide dismutase multigene family: a comparison of the CuZn-SOD (SOD1), Mn-SOD (SOD2), and EC-SOD (SOD3) gene structures, evolution, and expression, *Free Radic. Biol. Med.* 33 (2002) 337–349.
- [25] M. Maruyama, N. Kobayashi, K.A. Westerman, M. Sakaguchi, J.E. Allain, T. Totsugawa, T. Okitsu, T. Fukazawa, A. Weber, D.B. Stolz, P. Leboulch, N. Tanaka, Establishment of a highly differentiated immortalized human cholangiocyte cell line with SV40T and hTERT, *Transplantation* 77 (2004) 446–451.
- [26] Y. Hiraku, M. Murata, S. Kawanishi, Determination of intracellular glutathione and thiols by high performance liquid chromatography with a gold electrode at the femtomole level: comparison with a spectroscopic assay, *Biochim. Biophys. Acta* 1570 (2002) 47–52.
- [27] S. Soberanes, A. Gonzalez, D. Ulrich, S.E. Chiarella, K.A. Radigan, A. Osornio-Vargas, J. Joseph, B. Kalyanaraman, K.M. Ridge, N.S. Chandel, G.M. Mutlu, A. De Vizcaya-Ruiz, G.R. Budinger, Particulate matter Air Pollution induces hypermethylation of the p16 promoter via a mitochondrial ROS-JNK-DNMT1 pathway, *Sci. Rep.* 2 (2012) 275.
- [28] S. Laget, B. Miotto, H.G. Chin, P.O. Esteve, R.J. Roberts, S. Pradhan, P.A. Defossez, MBD4 cooperates with DNMT1 to mediate methyl-DNA repression and protects mammalian cells from oxidative stress, *Epigenetics* 9 (2014) 546–556.
- [29] D. Hanahan, R.A. Weinberg, Hallmarks of cancer: the next generation, *Cell* 144 (2011) 646–674.
- [30] M. Shipitsin, K. Polyak, The cancer stem cell hypothesis: in search of definitions, markers, and relevance, *Lab. Invest.* 88 (2008) 459–463.
- [31] S. Ohnishi, N. Ma, R. Thanan, S. Pinlaor, O. Hammam, M. Murata, S. Kawanishi, DNA damage in inflammation-related carcinogenesis and cancer stem cells, *Oxid. Med. Cell. Longev.* 2013 (2014) 387014.
- [32] Y. Jia, D. Wu, F. Yun, L. Shi, N. Luo, Z. Liu, Y. Shi, Q. Sun, L. Jiang, S. Wang, M. Du, Transforming growth factor-beta1 regulates epithelial-mesenchymal transition in association with cancer stem-like cells in a breast cancer cell line, *Int. J. Clin. Exp. Med.* 7 (2014) 865–872.
- [33] K. Uchibori, A. Kasamatsu, M. Sunaga, S. Yokota, T. Sakurada, E. Kobayashi, M. Yoshikawa, K. Uzawa, S. Ueda, H. Tanzawa, N. Sato, Establishment and characterization of two 5-fluorouracil-resistant hepatocellular carcinoma cell lines, *Int. J. Oncol.* 40 (2012) 1005–1010.